Mineralogical Magazine, October 1999, Vol. 63(5), pp. 743–755

Zn-spinel in the metamorphosed Zn-Pb-Cu sulphide deposit at Mamandur, southern India

P. K. CHATTOPADHYAY

Department of Geology, Jadavpur University, Calcutta-700032, India

ABSTRACT

At Mamandur, southern India, zincian spinel is associated with Zn-Pb-Cu sulphide ores, metamorphosed to the granulite facies. The Zn-spinel (X_{Zn} = 0.44–0.82) occurs in assemblages of: (a) cordierite + biotite + sillimanite + sphalerite + pyrite and/or pyrrhotite; (b) garnet + biotite + sphalerite + pyrite and/or pyrrhotite; (c) hornblende + biotite + sphalerite + pyrite and/or pyrrhotite; and (d) it also occurs in highly sheared quartz veins with sphalerite + pyrite/pyrrhotite. Two texturally and compositionally distinct modes of occurrence of Zn-spinel have been recorded from the metamorphic assemblages: one shows a polygonal, granular (equilibrium) fabric with Zn-spinel grains in textural equilibrium with cordierite in the granulite facies assemblage; the other which is involved in the formation of coronas in garnet- and hornblende-bearing assemblage of a younger paragenesis (presumably belonging to a late retrograde stage), shows distinct compositional zoning with depletion of Zn and enrichment in Fe and Mg from the rim inwards. A third mode of occurrence is as perfectly euhedral grains embedded in a quartzose matrix in quartz veins, often with sphalerite moulded over the Zn-spinel grains.

From textural evidence and consideration of stoichiometric balance, Zn-spinel occurring in association with cordierite is suggested to have formed by the prograde reactions: 0.46 biotite (Mg-rich) + 1.80 sillimanite + 3.01 quartz + 0.11 sphalerite = cordierite + 0.20 Zn-spinel + 0.80 K-feldspar + 0.06 pyrite + 4(OH,F) or 0.48 biotite (Mg-rich) + 2.08 sillimanite + 2.72 quartz + 0.26 sphalerite = cordierite + 0.50 Zn-spinel + 0.83 K-feldspar + 0.13 S_2 + 4(OH,F) and, the Zn-spinels occurring in association with garnet and hornblende by the retrograde reactions: garnet + 4.53 Al_2SiO_5 + 4.17 sphalerite = 5.38 Zn (-Fe)-spinel + 0.22 Ca-feldspar + 0.92 pyrite + 7.06 quartz + 1.23 S_2 and hornblende + 26.93 Al_2SiO_5 + 20.17 sphalerite + 0.88 pyrite = 25.93 Zn-spinel + 2 Ca-feldspar + 56.81 quartz + 11.32 S_2 + 2(OH,F) Zn-spinel in the sheared quartz vein may be of (meta-) hydrothermal origin. Formation of sphalerite through sulphurization of gahnite is ruled out on the evidence of the perfectly euhedral nature of the spinel and the absence of any breakdown product from the spinel.

KEYWORDS: Zn-spinel, sulphide metamorphism, granulites, prograde, retrograde, Mamandur, India.

Introduction

ZINCIAN spinel [$(Zn,Fe,Mg)Al_2O_4$] is found in a variety of geological settings, which include metamorphosed sulphide deposits, (e.g. Spry and Scott, 1986 *a,b*; Bristol and Froese, 1989; Bernier, 1990; Zaleski *et al.*, 1991), metamorphosed oxide-silicate deposits (Frondel and Klein, 1965), aluminous metasediments (e.g. Moore and Reid, 1989), pegmatites, quartz veins and greisens in metamorphic terrains (Spry and Scott, 1986*a*), marbles and skarns (Nemec, 1973), granite (Tulloch, 1981), contact metamorphic aureoles of plutons (Atkin, 1978) and as detrital grains in unconsolidated sediments (Bell, 1982). Besides its petrogenetic significance, the mineral has been recognized as a potential exploration guide for metamorphosed massive sulphides (Spry, 1984; Spry and Scott, 1986*a*) and sometimes even as a directional indicator (Sheridan and Raymond, 1984), i.e. a true pathfinder. Sphalerite and its derivatives (e.g. Sangster and Scott, 1976; Wall and England, 1979; Spry, 1984, 1987*a,b*), reactions involving primary/residual

zincite, breakdown of Zn-staurolite (e.g. Spry and Scott, 1986*b*; Moore and Reid, 1989; Bristol and Froese 1989; Zaleski *et al.*, 1991), and precipitation from a metahydrothermal solution are generally accepted as possible mechanisms of Zn-spinel formation during metamorphism.

At Mamandur, southern India, zincian spinel is restricted within the metamorphosed Zn-Pb-Cu sulphide ore zone in a variety of silicate (garnet, cordierite, hornblende and vein quartz) and sulphide-bearing assemblages. The silicate minerals show textural relationships (see later) suggesting reaction with sphalerite leading to the formation of Zn-spinel. However, two distinct modes of occurrence of Zn-spinel: (1) as a polygonal, granular (suggesting equilibrium) textured component of the prograde granulite facies assemblage involving cordierite, K-feldspar, biotite and sillimanite; and (2) as a component of coronas in garnet- and hornblende-bearing retrograde assemblages, suggest a complex reaction relationship.

The primary objective of the work is to study the petrogenetic significance of Mamandur Zn-spinel through understanding of specific prograde and retrograde metamorphic reactions that produced Zn-spinel and, then, to relate the two parageneses to specific stages of regional metamorphism of the area.

Geological setting

Mamandur is a small base-metal deposit metamorphosed to granulite facies within the well-known granulite terrain of southern India. The deposit is tabular and broadly conformable with the dominant NNE-trending foliation of the country rocks (Fig. 1). Two subzones can be recognized within the ore body: the hanging wall zone (0.66 m) has an average grade of Zn 5.88%, Pb 1.13%, Cu 0.54%, and Cd at 130 ppm and Ag at 40 ppm and the foot-wall zone (0.13 m) has an average grade of Zn 0.69%, Pb 0.12%, Cu 0.62% and Ag at 37 ppm (unpublished GSI Report, 1976–79).

The country rocks, apart from late noritic instrusions, are granulites, and can be broadly divided into two lithological units: (1) pyroxene granulites; and (2) pelitic and quartzo feldspathic gneisses. Pyroxene granulites are either garnetiferous or non-garnetiferous, the latter either an orthopyroxene-bearing granulite or a two-pyroxene (ortho + clino) granulite. Peletic and quartzo feldspathic gneisses comprise khondalite, leptynite and cordierite gneiss. Khondalites are a quartz, garnet and sillimanite gneiss with or without K-feldspar and are distinguished from quartzo-feldspathic gneiss or leptynite mainly by the presence of sillimanite. Cordierite gneiss

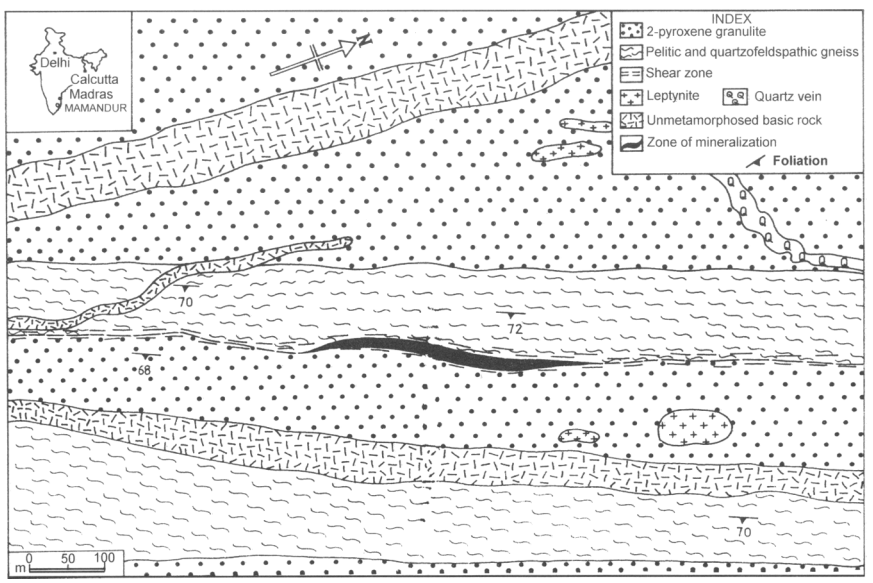

FIG. 1. Detailed map of the area around the ore zone, Mamandur. Note the stratiform, concordant nature of the mineralization.

TABLE 1. *P* and *T* estimated from the garnetiferous pyroxene granulite country rock

Sample	Thermobarometry	*T*°C (at 8.5 kbar)		*P* (kbar) (at 850°C)	
		Rim	Core	Rim	Core
155/G1O1P1	gt-opx-plag-qtz	818	764	8.5	7.8 (*P*Fe)
155/G202P2	gt-opx-plag-qtz	836	843	7.9	7.6 (*P*Fe)
156/G101	gt-opx	854	791		
154/G1C1	gt-cpx	805	810		
156/G1C1	gt-cpx	746	762		
155/G1C1P1	gt-cpx-plag-qtz	789	790	8.1	8.3 (*P*Hed)
155/G2C2P2	gt-cpx-plag-qtz	758	790	8.1	7.8 (*P*Hed)

Gt-opx thermometry: Lee and Ganguly (1988); gt-cpx thermometry: Ellis and Green (1979); gt-opx-plag-qtz barometry: Perkins and Chipera (1985); gt-cpx-plag-qtz barometry: Moechaar, *et al.* (1988)
*P*Fe = *P*(Ferrosilite)
*P*Hed = *P*(Hedenbergite)

forms lenses in the metapelites with a locally high MgO/FeO ratio. The ore is hosted by khondalite and cordierite gneisses in the foot-wall zone and by the same rocks with or without two-pyroxene granulite in the hanging wall zone.

Geothermobarometry and fluid activity

From thermobarometric investigation of the equilibrated silicate assemblages within the country rocks, the following salient features emerge:

(1) The maximum recorded temperature and pressure of metamorphism of the country rocks, obtained from the assemblages garnet-orthopyroxene-plagioclase-quartz (GOPS) and garnet-clinopyroxene-plagioclase-quartz (GCPS) systems are 850 (± 50)°C and 9 (± 0.5) kbar (Table 1). In the host-rock garnet-biotite is the only equilibrated assemblage from which temperature can be estimated. The Fe^{2+}–Mg partitioning between garnet and biotite is expressed by the reaction: pyrope + Fe-biotite = almandine + Mg-biotite. This exchange reaction has been used to formulate the garnet biotite thermometer by Thompson (1976). Ferry and Spear (1978) calibrated it empirically and Perchuk and Lavrent'eva (1983) by laboratory experiments. Later Ganguly and Saxena (1984) refined the Ferry and Spear (1978) thermometer incorporating the effect of non-ideality of garnet solid solution due to the effect of Ca and Mn. Dasgupta *et al.* (1991) developed a new formulation of garnet-biotite Fe-Mg exchange thermometer through statistical regression of the reversed experimental data of Ferry and Spear. The regression indicates that Fe-Mg mixing in biotite approximates a regular solution model showing positive deviation from ideality. Garnet-biotite thermometry from the host rock showed conspicuous variations (Table 2). These values fall into two clusters. The mean temperature corresponding to one cluster is 550°C and another

TABLE 2. Metamorphic temperatures (°C) obtained at 9 kbar using garnet-biotite thermometry from host rock.

Sample no.	Rim			Core		
	a	b	c	a	b	c
H69/G1B1	541	562	678	552	567	682
H16/G1B1	804	755	759	787	704	738
H16/G2B2	895	757	789	881	746	784
H66/G1B1	652	597	674	633	578	661
H8/G1B1	484	503	531	667	636	659
H140/G1B1	628	621	620	734	710	670
H140/G2B2	681	746	606	718	703	693
H67/G1B1	483	485	544	547	550	574
H67/G2B2	578	541	606	771	728	701
H78/G1B1	567	574	615	650	640	674
H64/G1B1	555	644	554	603	689	577
H64/G1B2	582	669	564	623	740	652
H17A/G1B1	512	628	518	634	747	565
H120/G1B2	787	805	662	821	827	679
H47A/G1				804	821	669

a: Ferry and Spear (1978)
b: Dasgupta *et al.* (1991)
c: Perchuk and Lavrent'eva (1983).

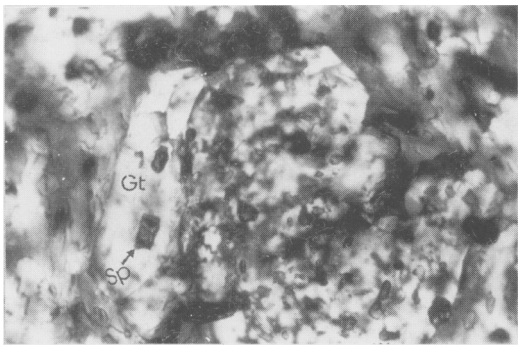

FIG. 2. A euhedral garnet (Gt) porphyroblast containing rounded sphalerite (Sp) inclusion trails arranged in a concentric zonal pattern. Other inclusions in the garnet are quartz, biotite and pyrite (PPL).

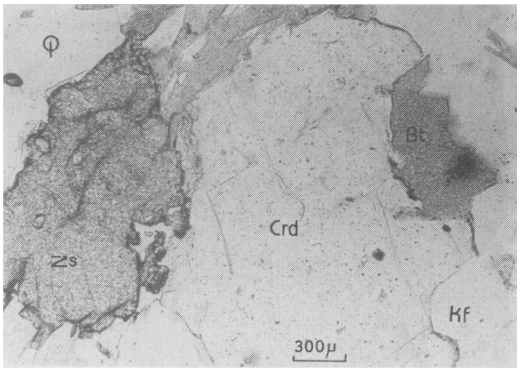

FIG. 3. Porphyroblastic Zn-spinel (Zs) and cordierite (Crd) are in mutual contact with a sharp automorphic grain boundary (top right). Q: Quartz Kf: K-feldspar (PPL).

850°C. The former probably represents the thermal field of retrogression. The higher values recorded are closer to those recorded from pyroxene granulites, thus the peak *T*. However, it is worthwhile to recall the limitations of this thermometer. Biotite compositions vary for several reasons. Spear (1991) showed that the variation in biotite composition depends on the amount of biotite in the rocks, the speed of cation diffusion in the matrix, and the proximity of a particular biotite grain to a garnet grain. The change in biotite composition, dependent as it is on mass proportion, would be insignificant where a large volume of biotite is involved, but substantial where a small proportion occurs.

(2) The *P-T-t* trajectory has been found to be an anticlockwise decompressive one where the prograde path and the decompressive path are well constrained (Chattopadhyay, 1996).

(3) Calculation of fluid activity from mineral–fluid equilibria at peak metamorphic conditions shows wide variation (0.16–0.68) in closely spaced outcrops suggesting that a H_2O gradient existed during peak metamorphism. Therefore the, 'pervasive CO_2-flux model' proposed by some workers for the amphibolite–granulite transition in the southern granulite belt (Pichamuthu, 1960; Janardhan *et al.*, 1982), is not valid here (Chattopadhyay, 1996).

Textural relations and their significance

Porphyroblastic and/or automorphic habits of several minerals (garnet, cordierite, spinel) in the observed assemblages produced some spectacular textural features that are genetically significant. For instance, sphalerite inclusion trails in a concentrically-zoned garnet porphyroblast (Fig. 2) or a Zn-spinel porphyroblast containing inclusions of sphalerite and hornblende (Fig. 10*a,b*) points not only to the pre-metamorphic existence of the sulphide ore minerals, but also indicates the paragenetic sequence among the prograde silicate minerals and the spinel. Sulphide-silicate reaction to produce Zn-spinel is documented in Fig. 7 (right) where sphalerite appears to have reacted with an adjacent garnet grain to produce the Zn-spinel while another nearby garnet grain (left) not in contact with sphalerite remains unchanged.

Zn-spinel occurs in four distinct petrographic assemblages: (a) cordierite (K-feldspar + sillimanite + biotite + quartz + sphalerite ± pyrite/pyrrhotite, chalcopyrite) -bearing rocks; (b) garnet (+ biotite + plagioclase + quartz + sphalerite ± pyrite/pyrrhotite, chalcopyrite) -bearing assemblage; (c) the hornblende (+ plagioclase + quartz + sphalerite ± pyrite/pyrrhotite, chalcopyrite, galena) -bearing assemblage; and (d) in highly sheared quartz veins (sphalerite ± pyrite, chalcopyrite, mackinawite). The textural relationship of Zn-spinel with the silicate minerals in the cordierite-bearing assemblage is strikingly different from those in the other three associations.

In the cordierite-bearing assemblage, Zn-spinel and cordierite porphyroblasts often occur in physical contact with sharp automorphic grain boundaries (Fig. 3, top right). Both cordierite and

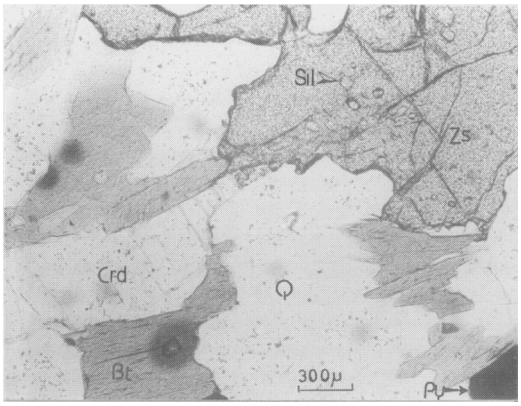

FIG. 4. A porphyroblastic Zn-spinel (Zs) grain includes blebs of sillimanite (Sil). A tabular cordierite (Crd) grain includes stout prisms of biotite (Bt). Py: Pyrite (PPL).

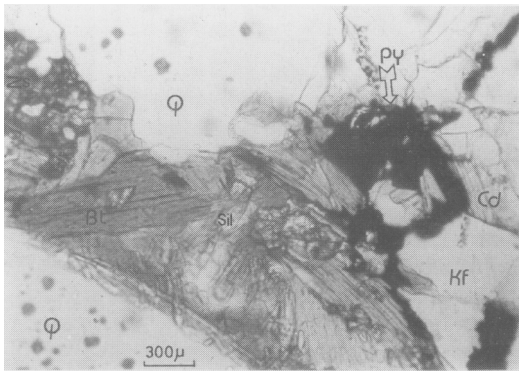

FIG. 5. The overall texture of the prograde assemblage of Zn-spinel (Zs), biotite (Bt), sillimanite (Sil), quartz (Q), porphyroblastic cordierite (Crd), K-feldspar (Kf) and pyrite (Py) (PPL).

Zn-spinel contain inclusions of sillimanite blades (Fig. 4), stout prisms of biotite and other silicates. Figure 5, shows a typical mineralogical assemblage. Overall, the granular polygonal texture of Zn-spinel, its sharp 'mutual boundary' contact against cordierite or other silicates, and the absence of any peripheral reaction rim point unequivocally to an equilibrium texture under a volatile-deficient granulite facies condition.

In contrast, Zn-spinel in the garnet bearing assemblage is generally anhedral or pseudomorphous after garnet (often retaining ghost relict cracks) and almost invariably associated with a partial or complete reaction-rim or 'corona' comprising calcic feldspar + quartz (Figs 6, 7, 8) ± sphalerite ± pyrite. The Zn-spinel grain boundaries are often serrated (unlike the previous case), as in Figs 6 and 7, suggesting dissolution.

In the hornblende-dominant assemblage, a corona comprising calcic plagioclase + quartz around Zn-spinel metacrysts is almost ubiquitous (Figs 9, 10*a,b*). Small grains of hornblende and

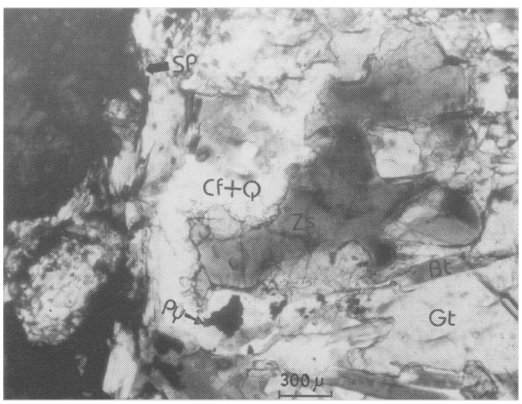

FIG. 6. A large porphyroblastic garnet (Gt) grain that contains prograde biotite (Bt), shows reaction relationship with an irregular shaped Zn-spinel (Zs) grain. The spinel grain is surrounded by a thin rim of Ca-feldspar (Cf) and quartz (Q). Pyrite (Py) is present close to the spinel grain (PPL).

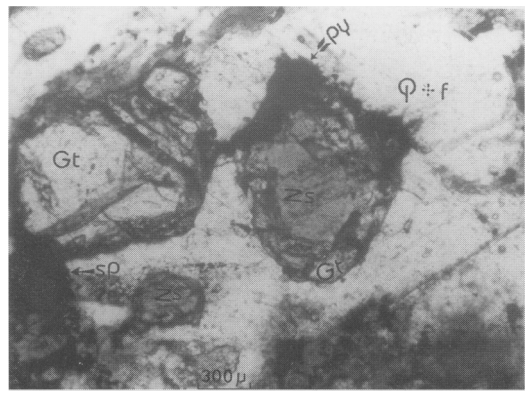

FIG. 7. Equant grains of garnet (Gt) in a quartzofelspathic (Q+F) matrix. One grain of garnet (right) in contact with sphalerite is replaced by Zn-spinel (Zs) while another (left) not surrounded by sphalerite, is unchanged. Sp: sphalerite (PPL).

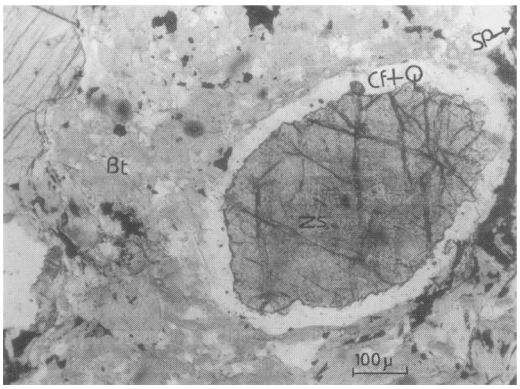

FIG. 8. An elliptical grain of Zn-spinel (Zs) pseudomorphous after garnet (inheriting its relict cracks) and surrounded by a thin rim of calcic-feldspar (Cf) and quartz (Q), which again is surrounded by a thin rim of sphalerite (Sp) and pyrite (Py) (PPL).

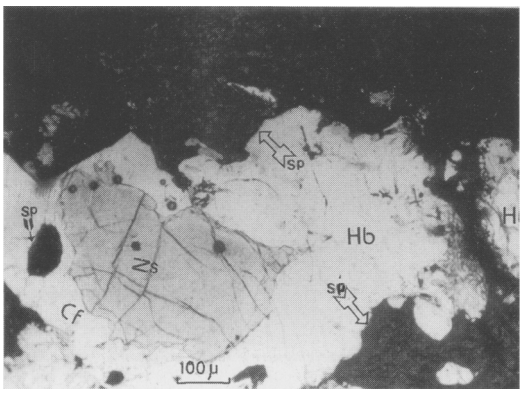

FIG. 9. A hornblende grain has been almost entirely replaced and pseudomorphed by Zn-spinel (Zs). A thin reaction rim of Ca-feldspar (Cf) and quartz (Q) surrounds the spinel grain. Sp: Sphalerite (PPL).

sphalerite are included (Fig. 10*a,b*) within Zn-spinel. Also of special significance is the scalloped nature of the sphalerite grain boundary against hornblende grain contact (Fig. 9) suggesting the possible activity of a fluid phase. That also explains why Zn-spinel is not always formed along the contact zone between reactants. Further indication of fluid activity at this stage comes from locally remobilized sphalerite and chalcopyrite along cracks and miocrofractures in the bulk rock.

In sheared quartz-veins which are free from any aluminosilicate mineral, coarse euhedral Zn-spinel grains are usually rimmed by sphalerite + pyrite (Fig. 11) and occur as disseminations in the quartz matrix. Sphalerite is often moulded over Zn-spinel grains (epitaxial growth?) (Table 3).

Textural evidence thus clearly indicates at least two generations of Zn-spinel. Those associated with cordierite show sharp polygonal outlines against cordierite; include the same set of prograde metamorphic minerals (stout prisms of biotite, sillimanite and K-feldspar) and common sulphides (sphalerite, galena, pyrite); and are entirely free from any reaction rim/corona texture. These are therefore prograde Zn-spinel formed under volatile-deficient peak metamorphic conditions. In contrast, Zn-spinel grains associated with garnet and hornblende are invariably rimmed by a fine-grained aggregate of quartz + Ca-plagioclase +

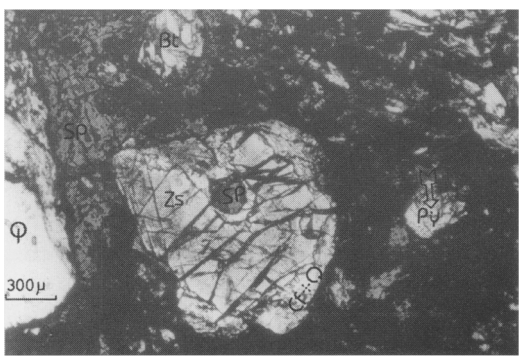

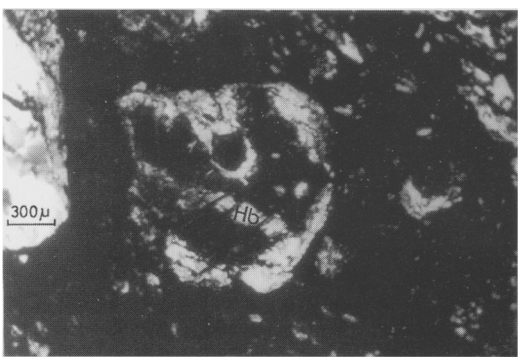

FIG. 10. (*a*) A Zn-spinel (Zs) grain with inclusions of hornblende (Hb) and sphalerite (Sp). A quartz (Q) plus Ca-feldspar (Cf) reaction rim surrounds the grain (PPL). (*b*) Same under crossed nicols.

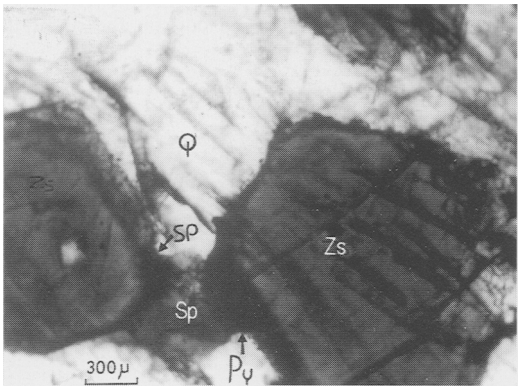

FIG. 11. Porphyroblastic euhedral Zn-spinel (Zs) in quartzose (Q) matrix. Sphalerite (Sp) (± pyrite (Py)) occurs as mantle (epitaxial overgrowth?) over the spinel grains (PPL).

pyrite; they often exhibit pseudomorphism after garnets and have serrated grain boundaries; it thus represents a sulphide–silicate reaction product under a retrograde, (relatively) volatile-enriched metamorphic conditions.

The texture of sheared vein quartz-associated Zn-spinel is inconclusive. The moulded sphalerite grains around perfect euhedra of Zn-spinel may represent hydrothermal precipitation reaction.

Overall, textural features thus indicate that Zn-spinel is essentially a product of silicate-sulphide (sphalerite) reactions in which the nature of co-products are determined by: (a) the composition of the reacting silicate minerals; and (b) by the *P-T-t* stage (prograde/retrograde) during which the reactions progressed.

Zincian spinel composition

Mineral analyses were carried out on an electron probe microanalyser model JEOL JXA 8600S at Roorkee University, India. Mineral compositions were determined by wavelength-dispersion spectrometry (WDS) using an accelerating voltage of 15 kV, a beam current of 10 nA and a beam diameter of 1–2 μm, against natural and synthetic mineral standards.

The composition of zincian spinel in samples from sulphide-rich rocks of Mamandur are shown in Table 4. Spinel with relatively low X_{Zn} (i.e. $Zn/(Zn+Fe^{2+}+Mg+Mn)$) in the range (0.44–0.51) and high X_{Mg} (0.17–0.21) and X_{Fe} (0.31–0.36) is associated with cordierite. Zincian spinel associated with garnet have X_{Zn} = 0.66–0.81, X_{Fe} = 0.11–0.21 and X_{Mg} = 0.06–0.15. Spinels associated with hornblende have X_{Zn} = 0.62–0.76, X_{Fe} = 0.13–0.21 and X_{Mg} = 0.08–0.17. Spinel grains in quartz veins have compositions close to those associated with garnet. The compositions of the cores of the spinels in terms of the 'end-members', hercynite, Zn-spinel and ortho-spinel, fall within the compositional field of spinels from metamorphosed massive sulphide deposits (Fig. 12)

TABLE 3. Textural features in Zn-spinel-sphalerite-silicate assemblages

Dominant silicate phase in the assemblage	Observed textural relationships
1. Cordierite-bearing	Sharp automorphic 'mutual boundary' texture between Zn-spinel and cordierite; both minerals contain inclusions of sillimanite, biotite, quartz, K-feldspar, sphalerite and pyrite. No, reaction rim/corona texture. Small Zn-spinel inclusions in cordierite implying its growth outlasting that of the spinel
2. Garnet-bearing	Zn-spinel anhedral or pseudomorphous after garnet; invariably rimmed, partially or completely, by quartz + Ca-feldspar + sphalerite + neocrystallized pyrite. Inclusions of lath-shaped primary biotite, sillimanite and sphalerite in garnet. Zn-spinel grain boundary serrated. Atoll-Zn-spinel inclusions (with corona) inside single garnet porphyroblast
3. Hornblende-bearing	Hornblende and sphalerite inclusions in Zn-spinel; ubiquitous corona of Ca-plagioclase + quartz around Zn-spinel metacrysts; deeply scalloped sphalerite grain boundary against hornblende; Zn-spinel inclusions (with corona) within hornblende also recorded.
4. Quartz veins	No definite sulphide-silicate reaction texture. Sphalerite, wherever present, occurs as 'moulded' epitaxially grown grains over Zn-spinel euhedra

TABLE 4. Average*, compositional variation of Zn-spinel in the rim and observed core in the different assemblages (only major components given)

	With cordierite (n = 2)		With garnet (n = 6)		With hornblende (n = 8)		With vein qartz (n = 2)	
	Rim	Core	Rim	Core	Rim	Core	Rim	Core
Al_2O_3	57.98	59.15	58.53	58.24	55.18	57.10	56.88	56.53
FeO	15.00	13.08	4.91	6.37	6.13	8.75	7.75	8.37
MnO	0.55	0.45	0.10	0.32	0.27	0.40	0.36	0.39
MgO	4.34	3.92	1.24	3.46	2.06	3.68	2.77	2.93
ZnO	20.00	23.68	36.31	32.44	33.16	27.76	29.91	30.98
Total	97.87	100.28	101.09	100.83	96.80	97.69	97.67	99.20
on the basis of 4 oxygen atoms								
Al	1.99	1.99	2.03	2.00	1.97	1.98	1.98	1.96
Fe^{2+}	0.35	0.30	0.12	0.15	0.13	0.20	0.17	0.17
Mn	0.01	0.01	0.002	0.008	0.006	0.01	0.01	0.01
Mg	0.19	0.17	0.05	0.15	0.09	0.16	0.12	0.13
Zn	0.43	0.50	0.77	0.68	0.74	0.60	0.66	0.67
X_{Fe}	0.36	0.30	0.13	0.15	0.13	0.20	0.18	0.18
X_{Mg}	0.19	0.17	0.05	0.15	0.09	0.17	0.13	0.13
X_{Mn}	0.01	0.01	0.00	0.01	0.01	0.01	0.01	0.01
X_{Zn}	0.44	0.52	0.82	0.69	0.77	0.62	0.68	0.68

n = number of grains analysed.
$X = i/(Fe^{2+} + Mg + Mn + Zn)$
* The detailed analyses of individual grains are available from the editor on request

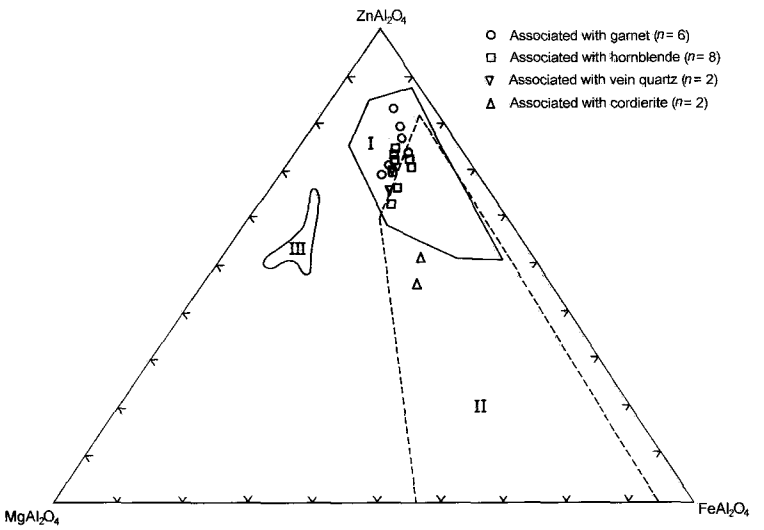

FIG. 12. Triangular plot showing the composition of zincian spinels from the Mamandur deposit in terms of $ZnAl_2O_4$–$FeAl_2O_4$–$MgAl_2O_4$ contents. Compositional fields of zincian spinel from known world wide occurrences of metamorphosed massive sulphides (I) and localities of aluminous metasediments (II) are indicated. (After Spry, 1984, and Spry and Scott, 1986*b*). Also shown are the composition of Zn-spinels from the granulite facies at Oranjefontein (III) (after Moore and Reid, 1989).

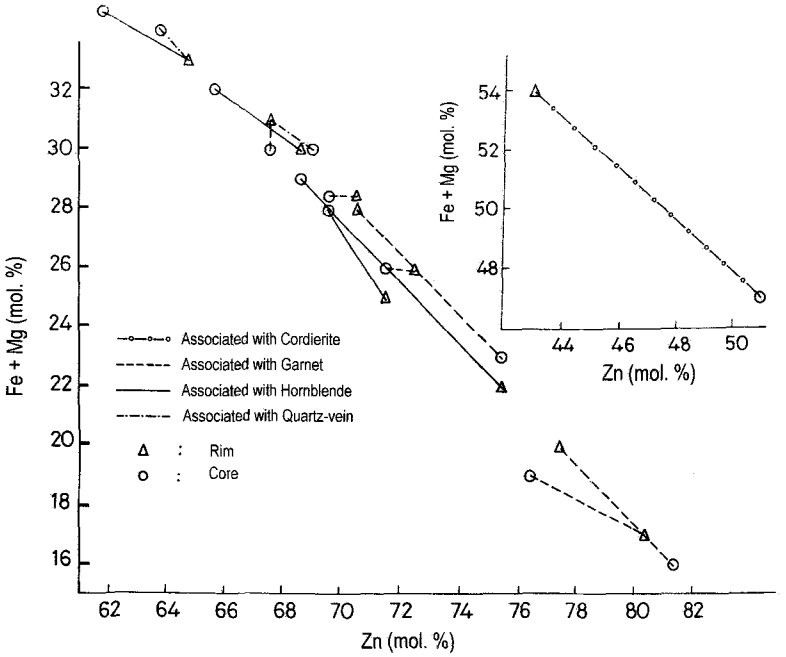

FIG. 13. Plot showing the variation in (Fe + Mg) *vs* Zn content in observed cores (circles), and rims (triangle) of individual spinel grains in different petrographic assemblages. Note the 'normal' and 'reverse' trends in prograde and retrograde spinels respectively (see text for discussion).

as compiled by Spry (1984) and Spry and Scott (1986*b*), except for the Zn-spinel grains associated with cordierite. The cordierite-associated spinel grains fall within the field of aluminous metasediments.

Spinel grains were checked for compositional zoning. Grains that were in contact with sphalerite showed significant enrichment of Zn at the rim, and were not considered. Only grains that are in contact with silicate phases are taken into consideration. The Fe+Mg mol.% *vs* Zn mol.% plot (Fig. 13) reveals the following features: (a) spinel grains associated with cordierite, show some increase in the Zn-spinel component and decrease in hercynite and spinel (*sensu stricto*), from the rim to observed core; (b) about 80% of the zincian spinel associated with garnet and hornblende, shows weak compositional zoning; (c) grains (n = 6) associated with garnet show a 3–4% decrease in the Zn-spinel component and a 2–3% increase in both hercynite and spinel (*sensu stricto*) components from rim to observed core; (d) grains (n = 5) associated with hornblende show the same phenomenon, with an up to 8% decrease in Zn-spinel and a 3–4% increase both in hercynite and spinel (*sensu stricto*), from rim to observed core; (e) quartz vein-associated spinel (n = 2) however, does not show any compositional zoning.

Probable reactions

From the textural relations where some of the reactants occur as (unconsumed) inclusions in the product phases and some products typically occur as coronas between reactant phases, and taking into consideration the 'average' core compositions of individual minerals, (i.e. biotite, cordierite, garnet, hornblende, Ca-feldspar and sphalerite – Table 5*a,b*) and Zn-spinel (Table 4), the following balanced reactions are suggested for the formation of Zn-spinel at Mamandur:

(a) The assemblage cordierite + Zn-spinel + biotite + quartz + sillimanite + sphalerite (Figs 3, 4, 5) suggests a reaction (assuming cordierite to be anhydrous):

0.462 biotite + 1.804 sillimanite + 3.016 quartz + 0.11 sphalerite = cordierite + 0.20 Zn-spinel + 0.80 K-feldspar + 0.06 pyrite + 4(OH,F) (1*a*)

TABLE 5*a*. Average chemical composition of dominant silicate phases associated with Zn-spinel

	Biotite (n = 12)		Cordierite (n = 3)		Garnet (n = 12)		Hornblende (n = 6)	
	rim	core	rim	core	rim	core	rim	core
SiO_2	39.15	38.50	48.86	48.78	38.23	38.47	48.73	48.11
TiO_2	0.78	0.80	b.d.	b.d.	b.d.	b.d.	0.23	0.21
Al_2O_3	19.05	18.68	32.02	31.94	21.53	21.59	8.52	8.68
Fe_2O_3 (T)	10.62	10.58	4.52	4.85	20.11	19.79	10.50	10.86
MnO	0.44	0.25	0.44	0.47	12.32	10.80	0.92	0.92
MgO	16.29	16.33	10.24	10.33	4.49	6.14	15.31	15.33
CaO	b.d.	b.d.	b.d.	b.d.	2.20	2.57	11.31	10.98
Na_2O	0.15	0.13	0.16	0.12	n.a.	n.a.	1.22	1.30
K_2O	9.97	9.86	b.d.	b.d.	n.a.	n.a.	0.52	0.47
Total	95.45	94.41	96.33	96.55	98.88	99.37	97.26	96.86
Oxygen basis	(24 O,OH,F,Cl)		18(O)		12(O)	12(O)	(24 O,OH,F,Cl)	
Si	5.62	5.60	5.15	5.04	3.01	3.02	7.04	7.02
Ti	0.08	0.08	b.d	b.d.	b.d	b.d.	0.025	0.022
Al^{IV}	2.38	2.40	3.90	3.89	2.00	1.99	0.96	0.97
Al^{VI}	0.85	0.80	b.d.	b.d.	b.d.	b.d.	0.52	0.50
Fe (T)	1.28	1.29	0.39	0.42	1.32	1.29	1.27	1.30
Mn	0.02	0.03	0.04	0.04	0.67	0.68	0.11	0.12
Mg	3.49	3.54	1.58	1.59	0.59	0.72	3.29	3.29
Ca	b.d.	b.d.	b.d.	b.d.	0.23	0.21	1.75	1.69
Na	0.04	0.04	0.03	0.02	n.a.	n.a.	0.34	0.36
K	1.83	1.82	b.d.	b.d.	n.a.	n.a.	0.10	0.09

The average chemical formulae of the dominant silicate phases are: biotite – $K_{1.82}(Mg_{3.54}Fe_{0.42})$ $(Al_{0.80}Ti_{0.08})$ $(Si_{5.6}Al_{2.4}O_{20})$ $(OH,F)_4$; cordierite – $Al_{3.0}(Mg_{1.59}Fe_{0.42})$ $(Si_{5.04}Al_{0.89}O_{18})$; garnet – $(Fe_{1.29}Mg_{0.72}Mn_{0.68}Ca_{0.21})$ $(Al_{1.79})$ $Si_{3.02}O_{12}$; hornblende – $(Na_{0.36}K_{0.09}(Ca_{1.69})$ $(Mg_{3.29}Fe_{1.30}Al_{0.30})(Si_{7.02}Al_{0.97}O_{22.17})(OH,F)_2$

or

0.48 biotite + 2.08 sillimanite + 2.72 quartz + 0.26 sphalerite = cordierite + 0.5 Zn-spinel + 0.83 K-feldspar + 0.13 S_2 + 4(OH,F) (1*b*)

(b) Zn-spinel in association with garnet + sphalerite and rimmed by Ca-feldspar (Table 5*b*) and quartz, (Figs 6, 7, 8) presumably formed by the reaction:

garnet + 4.53 Al_2SiO_5 + 4.17 sphalerite = 5.38 Zn-spinel + 0.22 Ca-feldspar + 0.92 pyrite + 7.06 quartz + 1.23 S_2
(assuming removal of excess Mn in the fluid phase) (2)

The Ca for the feldspar comes from the grossular content (5.27–12.75 mol.%) (Table 5*a*) of garnet. This is a modification of the reaction proposed by Spry (1987*b*) for the Aggeneys deposit, Namaqualand.

(c) Zn-spinel with hornblende (Table 5*a*) rimmed by Ca-feldspar (Table 5*b*) + quartz (Figs 9, 10, 11) suggest the reaction of hornblende and sphalerite in the presence of aluminosilicate. The reaction may be:

hornblende + 26.93 Al_2SiO_5 + 20.165 sphalerite + 0.88 pyrite = 25.93 spinel + 2 Ca-feldspar + 56.81 quartz + 11.32 S_2 + 2(OH,F)
(assuming removal of Na_2O and K_2O in the fluid phase) (3)

(d) Zn-spinel in quartz veins (Fig. 12) probably crystallized independently from the fluid phase and was moulded by sphalerite due to a change in the f_{S_2} condition of the fluid.

Petrogenetic implication

The hercynite and the gahnite components in a Zn-spinel in equilibrium with sphalerite are a function of P, T, the bulk chemistry and the ambient f_{O_2}–f_{S_2} conditions imposed by local

TABLE 5*b*. Average chemical composition of Ca-feldspar and sphalerite associated with Zn-spinel

	Ca-felds[1] (n = 7)	Ca-felds[2] (n = 3)		Sphalerite S1 (n = 13)	S2 (n = 10)	S3 (n = 8)
SiO_2	46.44	45.10				
TiO_2	b.d.	b.d.	FeS	5.91	5.79	5.50
Al_2O_3	34.14	35.08	ZnS	59.12	60.24	58.98
Fe_2O_3 (T)	b.d.	b.d.	CuS	0.36	0.20	0.09
MnO	b.d.	b.d.	S	35.64	33.28	35.29
MgO	b.d.	b.d.		2 cation basis		
CaO	17.26	18.42	Fe	0.10	0.09	0.09
Na_2O	1.61	1.20	Zn	0.86	0.89	0.85
K_2O	0.04	0.04	Cu	b.d.	b.d.	b.d.
Total	99.49	99.84	S	1.03	1.01	1.03
Oxygen basis	8(O)	8(O)				
Si	2.14	2.08				
Ti	b.d.	b.d.				
Al^{IV}	1.85	1.91				
Av^{VI}	b.d.	b.d.				
Fe (T)	b.d.	b.d.				
Mn	b.d.	b.d.				
Mg	b.d.	b.d.				
Ca	0.85	0.91				
Na	0.14	0.11				
K	0.002	0.002				

n = number of grains analysed from different samples
b.d. = below detection limit
Ca-felds[1] = coronal Ca-feldspar rimming Zn-spinel associated with hornblende
Ca-felds[2] = coronal Ca-feldspar rimming Zn-spinel associated with garnet
S1 = composition of sphalerite in the cordierite-bearing assemblage
S2 = composition of sphalerite in the garnet-bearing assemblage
S3 = composition of sphalerite in the hornblende-bearing assemblage

mineral assemblages. Similar also is the Zn-spinel–sphalerite equilibrium which is relatively insensitive to T and P (Spry and Scott, 1986*b*; Spry 1987*a*). Therefore in a situation where Zn-spinel + sphalerite coexists with pyrite and/or pyrrhotite and/or magnetite, and the temperature can be derived independently, f_{O_2} data can be retrieved readily for Zn-spinel ($\pm$ sphalerite) formation and equilibration. For instance, the Zn-spinel-magnetite-pyrite-pyrrhotite assemblage at the Black Mountain deposit (Spry , 1987*b*) points to buffering of f_{S_2} at $\sim 10^{-2.6}$ and f_{O_2} at $10^{-14.6}$ bars.

At Mamandur the Zn-spinel associated with cordierite has lower Zn and higher Mg and Fe compared to spinels in assemblages without cordierite. Here, cordierite is also Mg-rich (X_{Mg} = 0.8) relative to Fe (X_{Fe} = 0.2). Thus both spinel and cordierite point to a common FeMg-rich bulk precursor.

Two features of the composition of Zn-spinel from Mamandur merit special mention even though the data are scarce. Firstly, the bulk composition (Table 4) falls within the worldwide metamorphosed massive sulphides field (Fig. 12) of Spry (1984), except for those from quartz veins which fall in the field of aluminous metasediments; and secondly, there appears to be a first-order control of the chemical composition of reacting phases.

Thus, in the cordierite-bearing assemblage, high-Mg biotite breaks down to provide high Mg-cordierite plus relatively high-(Fe,Mg), Zn-deficient Zn-spinel with a small amount of pyrite.

The low Mg-Fe content in the reactant garnets (unlike the reactant biotite in the previous case) and further extraction of Fe by the product FeS phase enrich the spinel in Zn as it cannot be accommodated elsewhere. In the hornblende-associated reactions, the entire Mg,Fe content of hornblende plus the Fe-content of reactant pyrite plus the entire Zn,Fe contents of sphalerite are consumed only by the spinel phase, which therefore retains the same (Zn/Mg+Fe) ratio as in the bulk reactant. However such qualitative characterization is too simplistic, as in no circumstances are the reactants totally consumed and one has to deal with partitioning of chemical components within co-existing phase components – a process governed by f_{O_2}–f_{S_2}, P and T, besides the activities of the relevant chemical components. Calculated positions of the spinel-sphalerite equilibria in f_{O_2}–f_{S_2}–X space (accepting ideal behaviour along the $ZnAl_2O_4$–$FeAl_2O_4$ join) agree reasonably well with experimental results and theoretical calculation (Spry and Scott 1986*b*) which indicate that compositions of spinels in equilibrium with sphalerite plus pyrite/pyrrhotite become Zn-enriched with increasing f_{O_2} and f_{S_2} and thus can be used as an 'f_{O_2}-manometer' during metamorphism. Using their calibration curve (for 650°C, 5 kbar) (Fig. 8 in Spry and Scott 1986*b*) in the case of the garnet-affiliated Zn-spinel ($X_{Zn} = 0.67$), produced by reaction of sphalerite + aluminosilicate + pyrrhotite at Mamandur, $\log f_{O_2} = -19.1$ and $\log f_{S_2} = -5.5$ are obtained.

The other significant feature is the concentric compositional zoning of contrasted nature in prograde and retrograde Zn-spinel. Here again the data are scarce. However, the unquestionably prograde Zn-spinel produced in textural equilibrium with cordierite shows rather conspicuous Zn-enrichment from rim to core (Fig. 13), and all six (two superimposed) analyses from the decidedly retrograde, hornblende-bearing assemblage indicate a reverse zoning in terms of Zn *vs* (Fe+Mg) content. The relationship is inconclusive for garnet-associated Zn-spinels and almost constant in the case of Zn-spinel in quartz veins.

As Spry (1987*a*) has shown, $X_{gahnite}^{spinel}$ isopleths in P,T space show steeper positive slopes than a thermal gradient of 20°C/km, with successively higher values towards lower temperatures. Hence, during prograde porphyroblastic growth along any gradient steeper than 5°C/km, the Zn-spinel component for spinel in equilibrium with sphalerite-pyrrhotite (± pyrite) would decrease progressively. Reversal of such zoning would occur along any retrogression path with the same required gradient. The deduced patterns are consistent with observations in many metamorphosed sulphides deposits.

Acknowledgements

The author is grateful to the Geological Survey of India, Tamil Nadu Circle, for granting the field facilities. This work is a part of the author's Ph.D. thesis carried out under the guidance of Prof. S.C. Sarkar, to whom the author is grateful. Prof. A. Mookherjee and Prof. S. N. Dasgupta read an early draft of the paper and offered constructive suggestions. Dr Eva Zaleski is thanked for her critical comments and detailed review without which this work would have not been possible. A CSIR fellowship enabled the author to undertake the project and this is gratefully acknowledged.

References

Atkin, B.P. (1978) Hercynite as a breakdown product of staurolite from within the aureole of the Ardara pluton, County Donegal, Eire. *Mineral. Mag.*, **42**, 237–9.

Bell, H. (1982) Stratabound sulfide deposits, wall-rock alteration and associated tin-bearing minerals in the Carolina state belt, South Carolina and Georgia. *Econ. Geol.*, **77**, 294–311.

Bernier, L.R. (1990) Vanadiferous zincian-chromian hercynite in a metamorphosed basalt-hosted alteration zone, Atik Lake, Manitoba. *Canad. Mineral.*, **28**, 37–50.

Bristol, C.C. and Froese, E. (1989) Highly metamorphosed altered rocks associated with the Osborne lake volcanogenic massive sulfide deposit, Snow Lake area Manitoba. *Canad. Mineral.*, **27**, 593–600.

Chattopadhyay, P.K. (1996) *High grade metamorphism and the sulphidic ores at the Mamandur area, S. Arcot, Tamil Nadu, India.* Unpublished Ph.D. thesis. Jadavpur University, Calcutta, India, pp. 126–32.

Dasgupta, S., Sengupta, P., Guha, D. and Fukuoka, M. (1991) A refined garnet-biotite Fe-Mg exchange geothermometer and its application in amphibolites and granulites. *Contrib. Mineral. Petrol.*, **109**, 130–7.

Ellis, D.J. and Green, D.H. (1979) An experimental study of the effect of Ca upon garnet-clinopyroxene Fe-Mg exchange equilibria. *Contrib. Mineral. Petrol.*, **71**, 13–22.

Ferry, J.M. and Spear, F.S. (1978) Experimental

calibration of the partitioning of Fe and Mg between biotite and garnet. *Contrib. Mineral. Petrol.*, **66**, 113–7.

Frondel, C. and Klein, C., Jr. (1965) Exsolution in franklinite. *Amer. Mineral.*, **50**, 1670–80.

Ganguly, J. and Saxena, S.K. (1984) Mixing properties of aluminosilicate garnets: constraints from natural and experimental data, and applications to geothermobarometry. *Amer. Mineral.*, **69**, 88–97.

Janardhan, A.S., Newton, R.C. and Hansen, E.C. (1982) The transition from amphibolite facies gneiss to charnockite in southern Karnataka and northern Tamil Nadu. *Contrib. Mineral. Petrol.*, **79**, 130–49.

Lee, H.Y. and Ganguly, J. (1988) Equilibrium composition of co-existing garnet and orthopyroxene: experimental determinations in the system FeO-MgO-Al_2O_4-SiO_2 and applications. *J. Petrol.*, **29**, 92–113.

Moechaar, D.P., Essene, E.J. and Anovitch, L.M. (1988) Calculation and application of clinopyroxene-garnet-plagiocase-quartz geobarometers. *Contrib. Mineral. Petrol.* **92**, 92–106.

Moore, J.M. and Reid, A.M. (1989) A pan-African zincian staurolite imprint on Namaqua quartz-gahnite-sillimanite assemblages. *Mineral. Mag.*, **53**, 63–70.

Nemec, D. (1973) Das Vorkommen der Zn-Spinelle in der Böhmischen Masse, TMPM Tschermaks. *Min. Petr. Mitt.*, **19**, 95–109.

Perchuk, L.L. and Lavrent'eva, I.A. (1983) Experimental investigation of exchange equilibria in the system cordierite-garnet-biotite. In *Kinetics and Equilibrium in Mineral Reactions* (S.K. Saxena, ed.), Springer-Verlag, New York, pp. 199–240.

Perkins, D. and Chipera, S.J. (1985) Garnet-orthopyroxene-plagioclase-quartz barometry: refinement and application to the English River Subprovince at the Minnesota river valley. *Contrib. Mineral. Petrol.*, **89**, 69–80.

Pichamuthu, C.S. (1960) Charnockite in the making. *Nature*, **188**, 135–6.

Sangster, D.F. and Scott, S.D. (1976) Precambrian massive Cu-Zn-Pb sulfide ores of North America. In *Handbook of Strata-bound and Stratiform Ore Deposits* (K.H. Wolf, ed.), Elsevier, Amsterdam, **6**, pp. 129–222.

Sheridan, D.M. and Raymond, W.H. (1984) Precambrian deposits of zinc-copper-lead sulfides and zinc spinel (gahnite) in Colorado. *US Geol. Surv. Bull.*, **1550**, 31 pp.

Spear, F.S. (1991) On the interpretation of peak metamorphic temperatures in light of garnet diffusion during cooling. *J. metam. Geol.*, **9**, 379–88.

Spry, P.G. (1984) *The synthesis stability, origin and exploration, significance of zincian spinels.* Unpublished Ph.D. Thesis, Univ. Toronto, Ontario, Canada.

Spry, P.G. (1987*a*) Compositional zoning in zincian spinel. *Canad. Mineral.*, **25**, 97–104.

Spry, P.G. (1987*b*) The chemistry and origin or zincian spinel associated with Aggeneys Cu-Pb-Zn-Ag deposits, Namaqualand, South Africa. *Mineral. Deposita*, **22**, 262–8.

Spry, P. and Scott, S.D. (1986*a*) Zincian spinel and staurolite as guides to ore in the Appalachians and Scandanavian Caledonides. *Canad. Mineral.*, **24**, 147–63.

Spry, P. and Scott, S.D. (1986*b*) The stability of zincian spinels in sulfide systems and their potential as exploration guides for metamorphosed massive sulfide deposits. *Econ. Geol.*, **81**, 1446–63.

Thompson, A.B. (1976) Mineral reaction in pelitic rocks: II Calculation of some P-T-X (Fe-Mg) phase relations. *Amer. J. Sci.*, **282**, 1567–95.

Tulloch, A.J. (1981) Gahnite and columbite in an alkali-feldspar granite from New Zealand. *Mineral. Mag.*, **44**, 275–8.

Wall, V.J. and England, R.N. (1979) Zn-Fe spinel-silicate-sulfide reactions as sensors of metamorphic intensive variables and processes. *Geol. Soc. Amer. Abstracts with Program*, **V.11**, p. 354.

Zaleski, E., Froese, E. and Gordon, T.M. (1991) Metamorphic petrology of Fe-Zn- Mg-Al alteration at the Linda volcanogenic Massive sulfide deposit, Snow Lake, Manitoba. *Canad. Mineral.*, **29**, 995–1017.

[*Manuscript received 18 July 1997: revised 19 November 1998*]